Hearing Research 453 (2024) 109122

Contents lists available at ScienceDirect

Hearing Research

journal homepage: www.elsevier.com/locate/heares

Resting-state networks in chronic tinnitus: Increased connectivity between thalamus and visual areas

Tori Kok [a], Rosemary Varley [b], Chris Clark [c], Madeleine Verriotis [d], Kiran Seunarine [e], Giriraj Singh Shekhawat [f,*]

[a] Ear Institute, University College London 332 Gray's Inn Rd, London WC1X 8EE, UK
[b] Language & Cognition Chandler House 2 Wakefield Street London WC1N 1PF, UK
[c] Professor of Imaging and Biophysics, Clinical Systems Neuroscience, Developmental Neurosciences Research and Teaching Department, Great Ormond Street Institute of Child Health, University College London, 30 Guilford Street, London WC1N 1EH, UK
[d] Developmental Neurosciences Department UCL Great Ormond Street Institute of Child Health London, United Kingdom 30 Guilford Street London WC1N 1EH, UK
[e] Developmental Neurosciences Department UCL Great Ormond Street Institute of Child Health, Department of Neurosurgery Great Ormond Street Hospital for Children NHS Foundation Trust, 30 Guilford Street London WC1N 1EH, UK
[f] Dean (Research) EPSW, College of Education, Psychology and Social Work, Flinders University, Bedford Park, GPO Box 2100, Adelaide 5001, South Australia

ARTICLE INFO

Keywords:
Tinnitus
fMRI
Auditory connectivity
Resting-state networks

ABSTRACT

Tinnitus is thought to be associated with aberrant spontaneous activity in the central nervous system. Previous resting-state fMRI findings support this hypothesis and have shown a variety of alterations in neural activity in people with tinnitus compared to people without tinnitus. However, there is little replication of findings. Therefore, the current study aimed to extend on previous findings by investigating eight common resting-state networks (i.e. auditory, default mode, sensorimotor, visual, salience, dorsal attention, frontoparietal and language networks) using a control group ($n = 36$) and a group of tinnitus patients ($n = 46$) matched for age, sex and years of education. Hearing profiles matched up to 2 kHz and had a small but significant difference between groups in the high frequency range. Functional connectivity (FC) with dorsolateral prefrontal cortex (DLPFC) was also investigated separately for the first time, as this region is proposed to be core to tinnitus distress symptoms and most often used as a stimulation target in transcranial direct current stimulation (tDCS) research. The results showed that tinnitus patients had increased FC between bilateral thalamus and right visual association cortex compared to control participants. No differences were found with DLPFC, or with any of the resting-state networks (RSN), contrary to previous studies which have reported alterations in several RSNs.

1. Introduction

The exact mechanisms that underpin tinnitus, a phantom perception of sound affecting around 10 % of the population (Hackenberg et al., 2023), remain unclear. It has been proposed that tinnitus is caused by excessive spontaneous activity in the auditory pathway which is interpreted as a sound (Schaette and Kempter, 2006). Several models consider tinnitus pathology to be of central origin, including hyperactivity models such as thalamocortical dysrhythmia (TCD) (De Ridder et al., 2015; Llinás et al., 1999) and the frontostriatal gating model (Rauschecker et al., 2015). These models focus on hyperactivity in subcortical and cortical structures as opposed to the auditory periphery.

The TCD hypothesis suggests hyperpolarization of the medial geniculate body (MGB) results in a MGB firing mode-switch (Llinás et al., 1999). The frontostriatal gating hypothesis (Rauschecker et al., 2010) suggests tinnitus arises due to a break-down of limbic-auditory interactions at the level of the thalamus, or more specifically from MGB inhibition. Based on these models, one might expect increased connectivity between thalamus and auditory cortex. However, it could also be argued that decreased connectivity reflects the absence of gating activity.

If tinnitus is characterised by hyperactivity in central auditory areas, one would expect this hyperactivity to be detectable by brain imaging methods. As such, numerous studies have examined spontaneous brain activity using resting-state functional magnetic resonance imaging (rs-fMRI) in people with and without tinnitus. Kok et al. (2022) reviewed 29

* Corresponding author.
E-mail address: giriraj.shekhawat@flinders.edu.au (G.S. Shekhawat).

https://doi.org/10.1016/j.heares.2024.109122
Received 18 June 2024; Received in revised form 1 September 2024; Accepted 19 September 2024
Available online 4 October 2024

studies in a scoping review and found that 26 studies observed alterations in functional connectivity in people with tinnitus compared to those without. However, there was little consistency between studies regarding the nature of these alterations, with changes reported to several resting-state networks in tinnitus patients compared to controls, including but not limited to the auditory network (Berlot et al., 2020; Zhang et al., 2015), default mode network (DMN) (Job et al., 2020; Schmidt et al., 2017), attention networks (Burton et al., 2012; Schmidt et al., 2013), visual network (Chen et al., 2014; Maudoux et al., 2012), and limbic system (Chen et al., 2017a).

For auditory connectivity specifically, studies have found decreased as well as increased connections in auditory areas in roughly equal measures (Kok et al., 2022). For example, Berlot et al. (2020) found decreased connectivity between PAC and secondary auditory cortex as well as between PAC and MGB. Zhang et al. (2015) on the other hand found decreased connectivity between right thalamus and left superior temporal gyrus (STG), which is part of secondary auditory cortex.

The lack of replicability of findings is problematic and likely caused, in part, by the range of methodological decisions that need to be made when collecting and analysing fMRI data. As such, this study aimed to replicate findings from previous rs-fMRI studies by using the same regions-of-interest that have been used in previous studies. The regions were the core regions of several established resting-state networks. Beyond this, this study also aimed to investigate the connectivity of the dorsolateral prefrontal cortex (DLPFC) as this is the most frequently chosen target for transcranial direct current stimulation (tDCS) in tinnitus (Kok et al., 2021), whereas it has not specifically been used as a region-of-interest in previous research. This study also used a wider than usual range of audiological tests with the methods described in detail, and as such reports on a well-characterised group of tinnitus patients.

We formed three research questions. First, what do functional connectivity patterns between thalamus and auditory cortex look like in tinnitus patients compared to controls? We hypothesised we would find altered (i.e. either increased or decreased) functional connectivity between thalamus and primary auditory cortex (PAC) in the tinnitus group compared to the control group, as well as altered functional connectivity between PAC and secondary auditory cortices. As discussed in the introduction, studies have found both increased and decreased connectivity with auditory regions in tinnitus patients. Therefore, no specific prediction was held as to whether any alterations would be increased or decreased.

The second research question was to explore other resting-state networks such as the dorsal attention network and default mode network, based on a previous review showing several studies that found alterations in these networks (Kok et al., 2022).

The final research question was if functional connectivity with DLPFC is altered in tinnitus patients given the region's prevalence in tDCS research. No a priori hypothesis was held as this region has not been used as a seed in previous research.

2. Methods

2.1. Participant selection

The study was approved by the Research Ethics Committee of University College London, study ID: 17,601/001. All participants gave written informed consent. Participants with tinnitus were recruited through two charities, the British Tinnitus Association and Tinnitus Hub. Recruitment flyers were sent out through their social media and newsletters. Control participants were recruited by asking the tinnitus participants to bring a partner/friend/colleague with them to their appointment, where possible. Control participants were also recruited through the UCL psychology volunteer's portal, and through referrals from colleagues. The first appointment involved the questionnaires and hearing testing, and the second appointment involved the MRI scan which took place a couple of months apart due to availability constraints. All participants confirmed they still had chronic tinnitus at the time of the MRI scan.

Exclusion criteria for all participants were non-chronic tinnitus (< 6 months duration), pulsatile tinnitus, hyperacusis, deafness in one or both ears, profound hearing loss, Meniere's disease, and any MRI contraindications. Control participants should not have experienced frequent or chronic tinnitus, but occasional experience for short periods (e.g. after a concert) was acceptable. Unlike many previous studies which excluded participants with hearing loss to reduce confounding factors, the present study only excluded participants with profound hearing loss or deafness, as it is estimated that 70 – 85 % of tinnitus sufferers have hearing loss (Henry et al., 2005; Vernon and Meikle, 2000).

2.2. Participant characteristics

2.2.1. Demographics

A total of 84 participants were recruited (48 tinnitus participants and 36 control participants). Two participants from the tinnitus group (both male) were excluded because they exceeded the motion thresholds in their MRI scan. As such, the final control group consisted of 36 participants (19 female) and the final tinnitus group of 46 participants (19 female). Table 1 shows the participant demographics. Groups were matched for age, sex and years of education.

2.2.2. Hearing status

Pure tone audiometry was performed to record air conduction thresholds following BSA (British Society of Audiology) guidelines, with the addition of 6000 Hz and 12,000 Hz probes. Fig. 1 shows average pure tone audiometry thresholds of left and right ears combined for the tinnitus group compared to the control group (see Figure S2 and S3 in the supplements for average audiograms per group separately).

There was no difference in mean hearing thresholds between the groups at 250, 500, 1000, 2000, and 12,000 Hz. At 4000, 6000, and 8000 Hz, the tinnitus group had significantly higher thresholds ($p < 0.05$) on average than the control group (see Table S3 in the supplementary materials). However, the difference was small; around 10 dB on average.

Disregarding the 12,000 Hz thresholds (standard clinical practice for hearing loss diagnosis only tests up to 8000 Hz), for 14 control participants (39 %) all hearing thresholds were under 25 dB, indicating normal hearing at all frequencies. Only 2 participants with tinnitus (4 %) had normal hearing at all frequencies. The average hearing threshold (disregarding 12,000 Hz) was under 25 dB for 32 control participants (89 %) and for 36 tinnitus participants (78 %). Interestingly, only 16 participants with tinnitus (35 %) reported having a diagnosed hearing loss prior to testing, whereas in 44 participants with tinnitus some degree of hearing loss was present in their audiograms. Hearing loss in both groups followed the pattern of age-related, high-frequency hearing loss, which was mild-to-moderate in most participants. As to be expected, average pure tone thresholds correlated strongly to age in both groups, see Figure S4 in the supplementary materials.

Table 1
Demographics of participants. Data are presented as mean ± standard deviation. T-statistics are from independent samples *t*-tests with equality of variance assumed (Levene's test: all *p*'s > 0.05) for the age and years of education comparisons. For the sex comparison a chi-square test was performed.

	Tinnitus Group ($n = 46$)	Control Group ($n = 36$)	Group Comparisons
Age (years)	51.72 ± 11.62	52.11 ± 15.16	$t = 0.133$, $p = 0.894$
Years of Education	17.28 ± 2.95	16.89 ± 3.55	$t = -0.548$, $p = 0.585$
Sex	27 male/19 female	17 male/19 female	$\chi 2 = 1.069$, $p = 0.301$

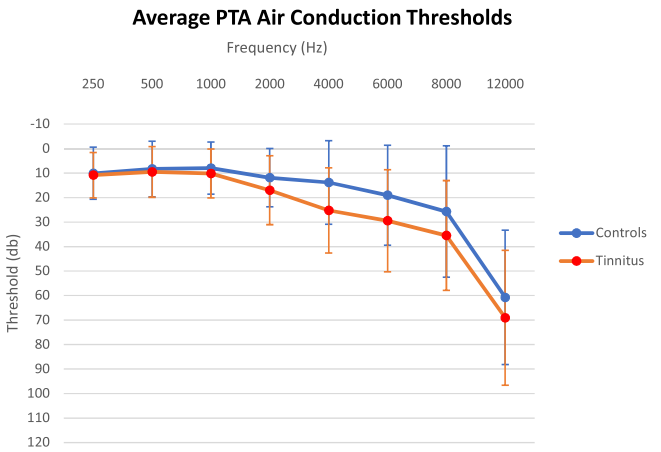

Fig. 1. Average pure tone audiometry (PTA) thresholds of both ears combined, comparing tinnitus and control groups. Difference between groups is significant ($p < 0.05$) for 4000 ($L + R$), 6000 ($L + R$), and 8000 (L) Hz (see Table S1). Error bars represent ± 1 SD.

Mean uncomfortable loudness levels (ULL) did not differ significantly between the two groups for low-frequency stimuli: 86.04 ± 10.90 (tinnitus) vs. 86.94 ± 11.38 (control) ($t = 0.364$, $p = 0.7168$) nor for high-frequency stimuli: 85.15 ± 13.12 (tinnitus) vs. 85.00 ± 12.58 ($t = 0.4010$, $p = 0.6895$).

2.2.3. Tinnitus characteristics

Tinnitus participants had tinnitus for an average of 8.7 years (SD = 10.22 years). The minimum duration was 8 months and the maximum duration was 46 years. The median tinnitus duration was 3.75 years. Participants reported a variety of tinnitus sounds: ringing ($n = 25$), hissing ($n = 25$), whistling ($n = 13$), buzzing ($n = 8$), static noise ($n = 7$), humming ($n = 4$), chirping ($n = 1$), ocean waves ($n = 1$). Thirty-nine participants reported their tinnitus was constant throughout the day, and seven reported it fluctuated. Tinnitus was reported in both ears ($n = 30$), centre of the head ($n = 9$), left ear ($n = 2$), right ear ($n = 3$), and back of the head ($n = 2$).

For full details on the audiometric testing procedures and outcomes, please see the supplementary materials. Tinnitus pitch matching using a forced-choice task (see Figure S1) showed most participants matched their tinnitus to a high-frequency sound. Eighty percent of the participants matched their tinnitus pitch to 4000 Hz or higher. Loudness matching showed the mean absolute tinnitus loudness was 40.48 dB (SD = 20.03) and the mean tinnitus loudness in sensation level was 10.5 dB (SD = 7.85). The mean absolute minimum masking level was 47.26 dB (SD = 17.9) and the mean minimum masking level in sensation level was 29.46 dB (SD = 16.64).

2.2.4. Questionnaire scores

All participants completed the following questionnaire assessments: Zung Self-Rating Depression Scale (SDS) (Zung, 1965), Zung Self-Rating Anxiety Scale (SAS) (Zung, 1971), and the Hyperacusis Questionnaire (HQ) (Khalfa et al., 2002). Tinnitus participants also completed the Tinnitus Handicap Inventory (THI) (McCombe et al., 2001) and the Tinnitus Functional Index (TFI) (Meikle et al., 2012).

Table 2 shows the results of the questionnaire measures completed by both groups. The tinnitus group had a significantly higher mean SAS and HQ score than the control group ($p = 0.027$ and $p = 0.01$, respectively). However, the mean difference in SAS was only 3.11 points on an 80-point scale and both mean scores are within the normal range. Similarly for the HQ, the mean difference was 3.6 points on a 42-point scale and both mean scores were within the normal range. There was no difference in SDS score.

The tinnitus group's tinnitus severity was mild-to-moderate on average as measured by the TFI and THI. Frequency distributions of TFI and THI scores can be found in supplementary Figures S5 and S6.

Table 2
Descriptive statistics for questionnaire measures. Data are presented as mean ± standard deviation. T-statistics are from independent samples *t*-tests with equal variances assumed (Levene's test all *p*'s > 0.05). * = $p < 0.05$ (2-tailed). SDS = Zung Self-Rating Depression Scale; SAS = Zung Self-Rating Anxiety Scale; HQ = Hyperacusis Questionnaire; THI = Tinnitus Handicap Inventory; TFI = Tinnitus Functional Index.

Questionnaire	Tinnitus Group	Control Group	Group Comparison
SDS	34 ± 8.56	32.22 ± 7.13	$t = -0.94$, $p = 0.35$
SAS	30.8 ± 6.85	27.69 ± 5.21	$t = -2.26$, $p = 0.027$*
HQ	12.04 ± 6.6	8.44 ± 5.36	$t = -2.66$, $p = 0.01$*
THI	30.65 ± 19.59	–	–
TFI	35.73 ± 22.77	–	–

2.3. MRI data acquisition

Scanning was conducted on a 3T Siemens Magnetom Prisma scanner with a 64-channel head coil at the Great Ormond Street Hospital in London, United Kingdom. The MRI acquisition consisted of a T1-weighted MPRAGE anatomical image (duration = 5 min, 21 s) with a voxel size of 1.0 × 1.0 × 1.0 mm^3. Other scanning parameters were repetition time (TR) = 2300 ms, echo time (TE) = 2.74 ms, inversion time (TI) = 909 ms, flip angle = 8°, in-plane matrix resolution = 256 × 256 mm, field of view = 256 × 256 mm, GRAPPA acceleration factor = 2.

This was followed by an interleaved resting-state fMRI acquisition (duration = 6 min, 18 s) using a T2*-weighted echo-planar pulse imaging (EPI) sequence with a voxel size of 2.5 × 2.5 × 2.5 mm^3. Other scanning parameters were TR = 1240 ms, TE = 26 ms, flip angle = 75°, 40 slices (2.5 mm thick), in-plane matrix resolution = 80 × 80 mm, field-of-view = 200 × 200 mm, 300 vol, and a multi-band acceleration factor = 2. An additional negative phase-encoded image (NEGPE) was acquired with the same parameters except for the phase-encoding direction, which was reversed (posterior-anterior), for the purpose of susceptibility distortion correction (acquisition time 7.5 s).

During the resting-state sequence, participants were instructed to look at a cross on the screen (white cross on a black background), stay awake, relax, and think of nothing in particular. During the T1-weighted scan participants had the option of watching or listening to anything they liked online. Participants wore ear plugs as well as over-ear headphones with padding to reduce audible noise from the MRI scanner as much as possible.

2.4. MRI data preprocessing

DICOM images were converted to NifTi format using Mrtrix3 (version: 3.0.3, https://www.mrtrix.org/). The first image from the resting-state fMRI time series was combined with the NEGPE image acquired directly afterwards, resulting in a pair of images with distortions in opposite directions. We applied FSL (version: 6.0.5.1) (Jenkinson et al., 2012) "topup" to the pair of images to estimate the susceptibility-induced off-resonance field, which was then used to remove the distortions from the full time series (Andersson et al., 2003; Smith et al., 2004). The raw images and new, corrected images were inspected side by side within FSLeyes (version: 1.3.0) (McCarthy, 2022). Dummy removal included removing the first four volumes of the resting-state acquisition.

Next, the data were preprocessed in SPM12 software (Statistical Parametric Mapping) (Friston et al., 2007) in the following order: motion correction through realignment of the functional images to a single reference image (the middle image was chosen as the reference image following recommendation in Poldrack et al. (2011)); coregistration of the structural image with the mean functional image; normalisation to

MNI-152 standard space; and spatial smoothing with a Gaussian kernel of FWHM = 6 mm. Normalisation was achieved by warping the individual anatomical and functional images into standard space using the DARTEL (Diffeomorphic Anatomical Registration Through Exponentiated Lie Algebra) toolbox in SPM (Ashburner, 2007). This required first segmenting the structural images to extract grey matter, white matter and cerebrospinal fluid images, and saving the DARTEL compatible native tissue images for each participant. All resulting warped images were inspected along with the MNI-152 template image to verify the accuracy of spatial normalisation. Participants with >2.0 mm or 2.0° displacements in the functional scans were excluded from analysis (Poldrack et al., 2011).

Next, the scans were imported to CONN software (RRID: SCR_009550) (version: 21) (Whitfield-Gabrieli and Nieto-Castanon, 2012). The functional data were de-noised in individual time series in MNI space. Eroded white matter and cerebrospinal fluid masks were used to regress out physiological noise from white matter and cerebrospinal fluid using CompCor (erosion level: 1) (Behzadi et al., 2007), to ensure full preservation of grey matter signal. The Artefact Rejection Toolbox (ART) in CONN was used to detect functional outliers for scrubbing (conservative settings, global signal z-value threshold = 3, subject-motion threshold = 0.5 mm). Then, linear regression of the following confounds was applied: motion (12 realignment parameters based on SPM12 preprocessing), physiological (comprising 5 WM and 5 CSF parameters), and scrubbing (for removal of outlier volumes identified with ART (range = 0 – 50 vol per participant).

The results of de-noising were inspected in CONN for each participant. Before de-noising, a histogram of the distribution of voxel-to-voxel connectivity values was skewed to the right and varied between participants. After de-noising, all histograms were centred around zero, with reduced inter-subject variability, indicating de-noising results were in line with expectation.

Finally, linear de-trending and a band-pass filter of 0.008 to 0.09 Hz (CONN default) was applied to the time series, to select the resting-state frequency band. The remaining fMRI signal was used for whole-brain seed-to-voxel functional connectivity analysis in CONN, i.e. correlating each seed of each network with all voxels in the brain.

2.5. Seed definition for functional connectivity analysis

To investigate resting-state networks (RSN) in tinnitus, the representative seeds for each RSN provided with CONN were selected. These seeds are based on the FSL Harvard-Oxford atlas, and they included the following: DMN (n = 4 seeds), sensori-motor network (n = 3 seeds), visual network (n = 4 seeds), salience network (n = 7 seeds), dorsal attention network (DAN) (n = 4 seeds), frontoparietal network (n = 4 seeds), and language network (n = 4 seeds).

To investigate auditory connectivity in tinnitus, four seeds were defined along the auditory pathway, based on the Harvard-Oxford atlas: left thalamus, right thalamus, left Heschl's Gyrus and right Heschl's Gyrus. To investigate DLPFC connectivity in tinnitus, the left and right DLPFC seeds from the CONN frontoparietal network were used. See Table 3 for detailed information on all seeds used in the analysis.

2.6. Statistical analysis of seed-based functional connectivity

2.6.1. Within-group analysis

For all participants and seeds of interest, a seed-to-voxel connectivity map was calculated in CONN. The resulting connectivity maps were visually inspected. Within-group analysis of auditory connectivity consisted of a one-sample t-test, while regressing for hearing loss as a covariate of no interest, for each of the four auditory seeds to find areas with significant functional connectivity to these seeds. A p-FDR corrected cluster threshold of $p < 0.05$ was used and a p-uncorrected voxel threshold of $p < 0.001$, which are the recommended default settings in CONN.

Table 3
Seed definition for functional connectivity analysis. mPFC = medial prefrontal cortex; PCC = posterior cingulate cortex; ACC = anterior cingulate cortex; PFC = prefrontal cortex; FEF = frontal eye field; IPS = intraparietal sulcus; DLPFC = dorsolateral prefrontal cortex; IFG = inferior frontal gyrus; pSTG = posterior superior temporal gyrus. Seeds in bold were investigated separately; the other seeds were combined in a network analysis (see 3.7.2) to reduce the number of individual analyses run.

Resting-state network	Seed	MNI Coordinates
Auditory network	**Left thalamus**	−9, −17, 6
	Right thalamus	10, −19, 6
	Left primary auditory cortex	−52, −19, 7
	Right primary auditory cortex	50, −21, 7
Default mode network	mPFC (anterior node)	1, 55, −3
	Left angular gyrus	−39, −77, 33
	Right angular gyrus	47, −67, 29
	PCC-precuneus (posterior node)	1, −61, 38
Sensorimotor network	Left premotor/supplementary motor area	−55, −12, 29
	Right premotor/supplementary motor area	56, −10, 29
	Primary motor area	0, −31, 67
Visual network	Primary visual area	2, −79, 12
	Secondary visual area	0, −93, −4
	Left visual association cortex	−37, −79, 10
	Right visual association cortex	38, −72, 13
Salience network	ACC	0, 22, 35
	Left anterior insula	−44, 13, 1
	Right anterior insula	47, 14, 0
	Left anterior PFC	−32, 45, 27
	Right anterior PFC	32, 46, 27
	Left supramarginal gyrus	−60, −39, 31
	Right supramarginal gyrus	62, −35, 32
Dorsal attention network	Left FEF	−27, −9, 64
	Right FEF	30, −6, 64
	Left IPS	−39, −43, 52
	Right IPS	39, −42, 54
Frontoparietal network	**Left DLPFC**	−43, 33, 28
	Right DLPFC	41, 38, 30
	Left posterior parietal cortex	−46, −58, 49
	Right posterior parietal cortex	52, −52, 45
Language network	Left IFG	−51, 26, 2
	Right IFG	54, 28, 1
	Left pSTG	−57, −47, 15
	Right pSTG	59, −42, 13

2.6.2. Between-group analysis

To compare auditory and DLPFC connectivity between the tinnitus and control group, whilst including hearing loss as a covariate of no interest, differential connectivity was calculated using a one-way ANCOVA with the contrasts [1 −1 0] (tinnitus, control, hearing threshold) for increased connectivity in tinnitus vs. control participants and [−1 1 0] (tinnitus, control, hearing threshold)for decreased connectivity in tinnitus vs. control participants. A two-sample t-test was also run with the contrasts [1 −1] and [−1 1] to investigate auditory functional connectivity without controlling for hearing loss. Analyses were run for each seed in bold separately as indicated in Table 3.

For the networks analysis, a single analysis was run per network by selecting all the seeds in the network to investigate regions functionally connected to any of the seeds (i.e. between-sources contrast had an "OR" structure, for example [0 1; 1 0]). The between-subjects contrasts used were [1 −1 0] and [−1 1 0] (with hearing loss as a covariate) and [1 −1] and [−1 1] (without hearing loss as a covariate), as in the auditory connectivity analysis. A p-FDR corrected cluster threshold of $p < 0.05$ was used in all analyses as well as a p-uncorrected voxel threshold of $p < 0.001$, which is the recommended default setting in CONN.

2.6.3. Correlation analysis with clinical characteristics

To investigate any potential relationship between functional connectivity and clinical characteristics of tinnitus patients, the mean z-

values (as per the whole-brain seed-to-voxel functional connectivity map created in CONN based on time-series correlation) for each tinnitus participant were extracted for regions showing significant differences between the tinnitus and the control group. These z-values were exported to SPSS 27.0 for Pearson correlation analysis with the following clinical characteristics: tinnitus duration (in months), THI score, TFI score, HQ score, SDS score, SAS score, tinnitus loudness match in absolute and sensation level, and mean hearing threshold for both ears combined. Partial correlations were calculated with age and years of education as controlling variables. Bonferroni correction was applied to correct for multiple comparisons in the correlation analysis by using a corrected alpha-threshold of 0.0025 ($\alpha = 0.05/20$).

3. Results

3.1. Functional connectivity results

3.1.1. Within-group analysis

The results of the within-group analysis using four seeds, i.e. bilateral Heschl's gyrus and bilateral thalamus, are depicted in Figs. 2 and 3A, respectively. In both groups, within-group analysis with Heschl's gyri seeds showed widespread bilateral functional connectivity with auditory regions, pre- and postcentral gyrus, cingulate gyrus, precuneus, and insular cortex, amongst others. For thalamus seeds, both groups showed widespread bilateral functional connectivity with precuneus, cingulate gyrus, pre- and post-central gyrus, paracingulate gyrus, and insular cortex, amongst others.

3.1.2. Between-group analysis

The differential functional connectivity (FC) analysis between the tinnitus and the control groups (Tinnitus > Control) found increased FC for both left thalamus and right thalamus. Fig. 3B and Table 4 show this result. When hearing loss was not included as a covariate in the analysis, the tinnitus group in comparison to the control group showed significantly increased FC between the left thalamus and a cluster in right visual association cortex. Similarly, right thalamus also showed significantly increased FC with a cluster in right visual association cortex again in the tinnitus group compared to the control group.

When hearing loss was included as a covariate, these significant clusters did not survive the p-uncorrected threshold of $p < 0.001$. However, the result could be recovered by making the threshold more lenient (also see Fig. 3B): $p < 0.0095$ for left thalamus seed, and $p < 0.00103$ for right thalamus seed. This suggests the difference in thalamic FC with right visual association cortex in tinnitus patients compared to controls is related partly to the tinnitus patients' having higher hearing thresholds. However, the result is still borderline significant after controlling for hearing loss, suggesting the difference is at least in part driven by the Tinnitus vs. Control contrast.

No differences in FC were found between the groups using bilateral Heschl's gyrus or bilateral DLPFC as seeds, or using any of the combined network seeds as shown in Table 3, whether hearing loss was included as a covariate or not. Also, no decreased connectivity was found in the tinnitus group compared to controls.

3.1.3. Correlation analysis with clinical characteristics

The z-values for significant clusters in the between-group analysis were extracted for each tinnitus participant to investigate any relationship with tinnitus clinical characteristics. The z-values for FC between left thalamus and right visual association cortex, as well as between right thalamus and right visual association cortex, were not significantly correlated to any of the clinical measures, with or without Bonferroni correction. Table S4 in the supplementary materials shows

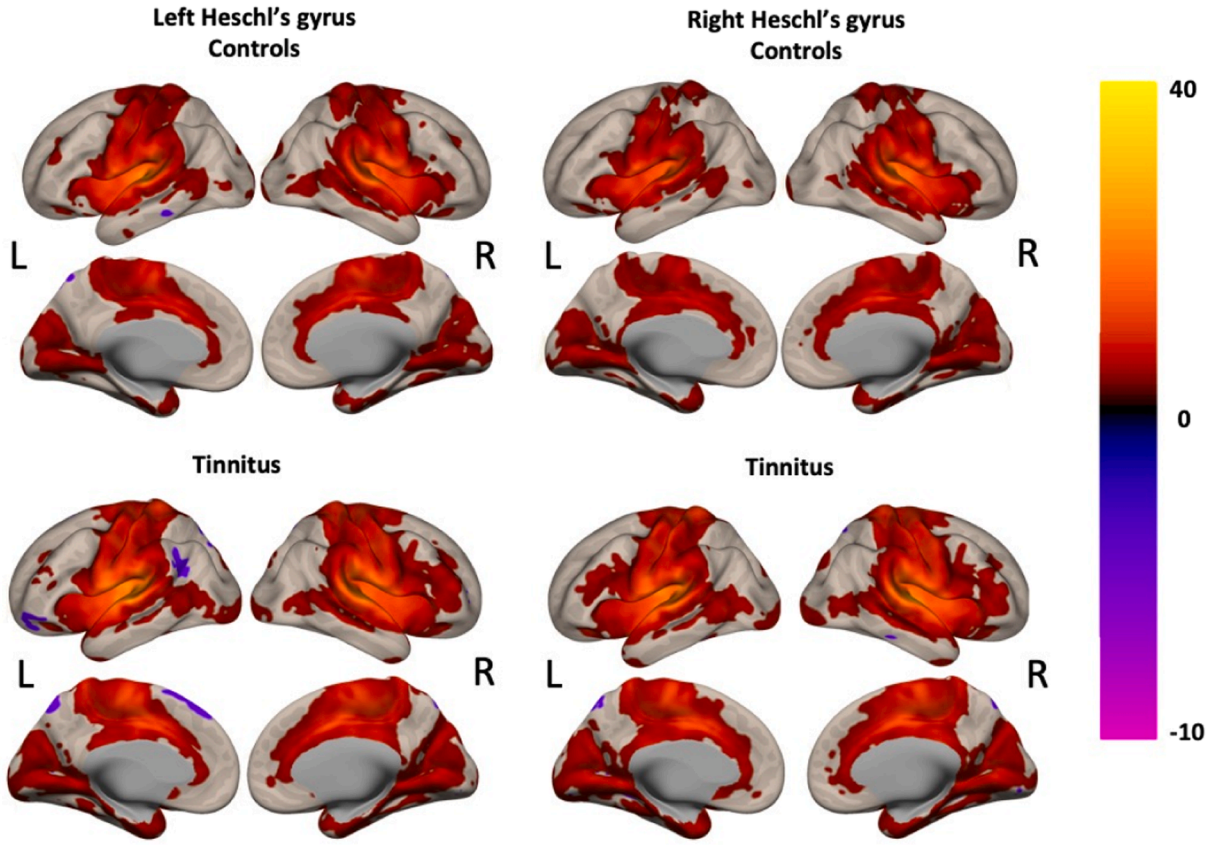

Fig. 2. Within-group functional connectivity analysis using left Heschl's gyrus and right Heschl's gyrus as seeds for the control group (top) and tinnitus group (bottom). *L* = left hemisphere view, *R* = right hemisphere view.

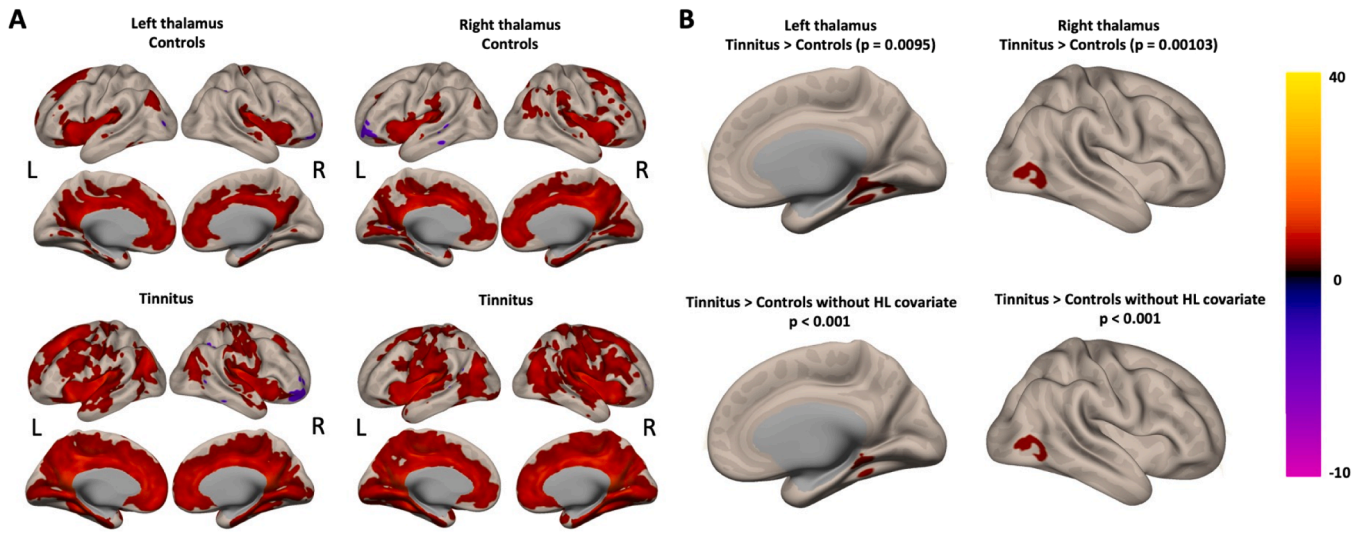

Fig. 3. A: Within-group functional connectivity analysis using left thalamus and right thalamus as seeds for control group (top) and tinnitus group (bottom). B: Between-group analysis comparing tinnitus and control group using left and right thalamus as seeds while controlling for hearing loss (top) and without controlling for hearing loss (bottom). *L* = left hemisphere view, *R* = right hemisphere view. The p-value refers to the p-uncorrected voxel threshold used in the statistical analysis.

Table 4
Results from Tinnitus > Controls (contrast: [1 −1]) functional connectivity analysis with left thalamus and right thalamus as seeds in tinnitus patients compared to controls without hearing loss as a covariate.

Seed	Brain regions	BA	MNI coordinates cluster peak	Statistics	Extent
Left thalamus (−9, −17, 6)	Right visual association cortex	19	+18, −46, −10	$t = 4.06$, $p < 0.001$	137 voxels
Right thalamus (10, −19, 6)	Right visual association cortex	19	+58, −68, +06	$t = 3.76$, $p < 0.001$	154 voxels

the results of the Pearson correlation analysis.

4. Discussion

This study aimed to expand on the evidence from previous studies that tinnitus patients have altered functional connectivity in resting-state networks compared to non-tinnitus participants. Using seeds in the most common resting-state networks provided with CONN, this study found no evidence for widespread alterations to resting-state networks. Visual inspection of Fig. 2 suggested that functional connectivity was more widespread in the tinnitus group. However, this was not confirmed by the between-group analysis. The exception was a finding of increased functional connectivity between bilateral thalamus and right visual association cortex in the tinnitus group compared to a control group that was well-matched for age, sex, and years of education. This finding was not associated with any clinical tinnitus characteristics, as shown in the correlation analysis, but was dependent on hearing status: when controlling for hearing status by including hearing loss as a covariate in the analysis, the finding became only borderline significant, whereas it was significant when uncontrolled for hearing loss.

This raises the question whether the finding is explicable by hearing differences between the groups, by the presence of tinnitus, or both. This study did not exclude participants with hearing loss, contrary to many previous studies. It is estimated that around 70 – 85 % of those with tinnitus have hearing loss (Henry et al., 2005; Vernon and Meikle, 2000). Therefore, excluding this group leads to results that are not representative of the tinnitus population at large and is focusing on the exception rather than the standard profile. However, this does present the issue of controlling for hearing loss in the data. Every effort was made to match the tinnitus and control groups on hearing status, but despite matching the average age of participants, the tinnitus participants' hearing thresholds on high-frequency tones were ±10 dB higher than those of the control participants.

As the result of increased functional connectivity between bilateral thalamus and right visual association was still borderline significant after controlling for hearing status, and the correlation analysis found no association between hearing status and the functional connectivity strength (z-scores) in the tinnitus group, it is fair to assume the result is not entirely driven by the 10 dB average difference in hearing status between the groups. However, the present analysis is unable to identify an interaction effect between tinnitus status and hearing status. Future research might want to consider a factorial analysis which takes into account both, as previous research suggests interaction effects between the two might exist. For example, visual cortex has been implicated in groups where tinnitus and a marked hearing loss exist, and less so in groups with tinnitus but no hearing loss (Vanneste et al., 2019).

The question remains what is driving the difference observed, as no association was found with any of the other clinical tinnitus characteristics. Altered functional connectivity between thalamus and visual areas in tinnitus participants is not a novel finding. Indeed, several other studies have observed functional connectivity differences between these regions.

Zhang et al. (2015) used left thalamus and right thalamus as seeds in their analysis of thalamocortical functional connectivity in 31 tinnitus patients and 33 controls matched for age, sex, and education, and all participants had normal hearing. They found decreased functional connectivity between right thalamus and left middle occipital gyrus, the peak MNI coordinates (−48, −72, 15) corresponding to visual association cortex. This is opposite to the finding of increased FC between right thalamus and visual association cortex found in the present study. Similarly, Zhang et al. (2015) did not find an association with clinical tinnitus characteristics and their result. However, they observed other alterations in FC that were correlated to tinnitus measures. Right thalamus showed decreased FC with left superior temporal gyrus (auditory cortex), which was negatively correlated with tinnitus duration ($r = -0.454$, $p = 0.017$). Left thalamus showed decreased FC with right

middle temporal gyrus (secondary auditory cortex), which was negatively correlated with Tinnitus Handicap Questionnaire total score ($r = -0.482$, p – 0.011).

Chen et al. (2023) compared the resting-state FC of the thalamus in tinnitus patients who had different outcomes after sound therapy and with controls. Between the tinnitus groups and the controls, they found altered FC with areas of the striatal network, auditory-related cortex, and the limbic system. They also found decreased FC with the right cuneus, a part of the occipital lobe involved in visual processing. They suggest that functional changes between the thalamus and cuneus may result from multisensory interactions between auditory and visual regions in tinnitus. The salience of the tinnitus perception might decrease spontaneous activity in visual regions (Chen et al., 2015b), Chen et al. (2017b).

Chen et al. (2023) also found significantly increased fractional amplitude of low-frequency fluctuation (fALFF) in the whole thalamus, right parietal area, bilateral prefrontal region, and the left visual area. Interestingly, in a previous study, they found decreased amplitude of low-frequency fluctuations (ALFF) values in bilateral thalamus and in visual areas (Chen et al., 2014). They speculated this could be related to the decreased FC between auditory and visual areas observed in other studies (Burton et al., 2012; Maudoux et al., 2012).

The evidence taken together suggests that FC between thalamus and visual regions could be altered in tinnitus, but it is unclear why in some studies it is decreased (Chen et al., 2023; Zhang et al., 2015), but increased in the current study.

The thalamus regulates the flow of sensory information to and from the auditory cortex and plays an important role in tinnitus models such as the frontostriatal gating model (Rauschecker et al., 2010). According to this model, the thalamus mediates a noise-cancellation system consisting of limbic-auditory connections, and a failure of this mechanism results in tinnitus. Other models such as the thalamocortical dysrhythmia model (De Ridder et al., 2015; Gault et al., 2018) also propose that alterations to signal transmission at the level of the thalamus cause tinnitus. Based on these theories, one would predict altered FC between thalamus and other auditory regions or between thalamus and limbic regions. The current study hypothesised such changes, but only found changes between thalamus and visual regions. Therefore, this study found evidence in support of a role for the thalamus in tinnitus perception, although this did not align exactly with any specific tinnitus models.

Changes to the visual resting-state network in tinnitus have been observed in several studies (Burton et al., 2012; Chen et al., 2014; Chen et al., 2015a; Maudoux et al., 2012; Zhang et al., 2015), and all these studies viewed these changes as secondary effects to tinnitus rather than changes that could be driving the tinnitus percept itself. Due to the correlational nature of functional connectivity analysis no claims on causality can be made. One explanation is that of anti-correlation between the visual and auditory modality: activation in one system suppresses that in the other (Burton et al., 2012). Indeed, using MEG in a non-tinnitus group of healthy subjects, Molloy et al. (2015) showed that when participants were engaged in a visually demanding task, auditory responses were attenuated, supporting a neural account of shared audiovisual resources. The increased FC between thalamus and visual areas could reflect an increase in such an inhibitory mechanism through the cognitive load placed by constant tinnitus perception.

This study also aimed to investigate resting-state connectivity with DLPFC, the most chosen site of stimulation in tDCS research (Kok et al., 2021). No differences were found in functional connectivity between tinnitus and control groups using DLPFC as a seed. This was the first study to investigate DLPFC specifically. One study did investigate the functional connectivity of the frontoparietal resting-state network, of which DLPFC is a part. Job et al. (2020) used the frontoparietal network seeds in CONN, as in the present study, consisting of bilateral DLPFC and bilateral posterior parietal cortex. They found increased FC between the frontoparietal network and the right middle frontal gyrus, but it is not clear which seed in the frontoparietal network was driving the result from their reporting. Therefore, currently there is no evidence available from rs-fMRI research to support DLPFC as a region of special interest in tinnitus. It seems likely that positive results found in tDCS trials for tinnitus using DLPFC as a target might be non-specific to tinnitus, but rather share commonality with other conditions affecting emotional systems. Indeed, tDCS of DLPFC has been used in the treatment of depression and pain disorders with some positive results as well (Lefaucheur, 2016).

Finally, some limitations of this study should be mentioned. This study did not categorise the tinnitus group into smaller subgroups. For example, the five participants with unilateral tinnitus were not regarded in separation from the participants with bilateral or centre of the head tinnitus. A post-hoc analysis was performed in which the analysis presented in Table 4 was replicated, with the exception that the five unilateral tinnitus participants were removed from the analysis. The result using left thalamus as a seed was the same whether they were excluded or not, with peak MNI coordinates unchanged although the number of voxels implicated was reduced slightly ($n = 109$ instead of $n = 137$). The result using right thalamus as a seed was borderline significant in this post-hoc analysis with again the same peak MNI coordinates (uncorrected p-threshold = 0.0015 instead of 0.001); cluster size = 148 voxels instead of 154).

The tinnitus group also included a spectrum of tinnitus severity scores as measured by the THI and TFI. It was chosen to investigate the tinnitus group as a whole, to power the analysis appropriately, as subgrouping would have led to underpowering the analysis. Additionally, this study aimed to find neural correlates that apply to the tinnitus population more broadly rather than those specific to a subgroup of the tinnitus population, which also motivated the decision to include participants with or without hearing loss. Future studies might want to focus on a specific subgroup of the tinnitus population.

Additionally, it is difficult with all MRI research to control for any confounding effects from the scanner noise. All participants were given ear plugs and padded headphones to reduce noise interference. However, future studies might want to consider a post-scan questionnaire to identify whether the participants had a similar experience of the MRI noise. It may be the case that people with tinnitus are more bothered by scanner noise than others. Although the study excluded those with hyperacusis, and none of the participants verbally reported any discomfort from the scanner noise to the experimenter, a post-scan questionnaire might help to bring more confidence to any auditory studies using MRI.Conclusion

The present study found increased functional connectivity between bilateral thalamus and right visual association cortex in tinnitus patients compared to controls. No alterations were found using the common resting-state networks in CONN. Furthermore, no differences in functional connectivity were found with DLPFC as a seed. Taken together, the increased thalamus FC is in line with tinnitus models that postulate a role for thalamic hyperactivity in tinnitus perception. A neural account of shared resources between auditory and visual networks could potentially explain the result.

Author statement ethical statement

The study was approved by the Research Ethics Committee of University College London, study ID: 17,601/001. All participants gave written informed consent.

Hereby, I (Tori Kok) consciously assure that for the manuscript the following is fulfilled:

1) This material is the authors' own original work, which has not been previously published elsewhere.
2) The paper is not currently being considered for publication elsewhere.

3) The paper reflects the authors' own research and analysis in a truthful and complete manner.
4) The paper properly credits the meaningful contributions of co-authors and co-researchers.
5) The results are appropriately placed in the context of prior and existing research.
6) All sources used are properly disclosed (correct citation). Literally copying of text must be indicated as such by using quotation marks and giving proper reference.
7) All authors have been personally and actively involved in substantial work leading to the paper, and will take public responsibility for its content.

CRediT authorship contribution statement

Tori Kok: Writing – review & editing, Writing – original draft, Visualization, Project administration, Methodology, Investigation, Formal analysis, Data curation, Conceptualization. **Rosemary Varley:** Writing – review & editing, Supervision, Methodology, Conceptualization. **Chris Clark:** Writing – review & editing, Supervision, Software, Resources, Methodology, Funding acquisition, Conceptualization. **Madeleine Verriotis:** Writing – review & editing, Validation, Methodology. **Kiran Seunarine:** Writing – review & editing, Validation, Methodology. **Giriraj Singh Shekhawat:** Writing – review & editing, Supervision, Resources, Funding acquisition, Conceptualization.

Data availability

The data that has been used is confidential.

Supplementary materials

Supplementary material associated with this article can be found, in the online version, at doi:10.1016/j.heares.2024.109122.

References

Andersson, J.L., Skare, S., Ashburner, J., 2003. How to correct susceptibility distortions in spin-echo echo-planar images: application to diffusion tensor imaging. Neuroimage 20, 870–888.

Ashburner, J., 2007. A fast diffeomorphic image registration algorithm. Neuroimage 38, 95–113.

Behzadi, Y., Restom, K., Liau, J., Liu, T.T., 2007. A component based noise correction method (CompCor) for BOLD and perfusion based fMRI. Neuroimage 37, 90–101.

Berlot, E., Arts, R., Smit, J., George, E., Gulban, O.F., Moerel, M., Stokroos, R., Formisano, E., De Martino, F, 2020. A 7 Tesla fMRI investigation of human tinnitus percept in cortical and subcortical auditory areas. Neuroimage-Clin. 25, NA.

Burton, H., Wineland, A., Bhattacharya, M., Nicklaus, J., Garcia, K.S., Piccirillo, J.F., 2012. Altered networks in bothersome tinnitus: a functional connectivity study. BMC Neurosci. 13, NA.

Chen, Q., Lv, H., Wang, Z., Li, X., Wang, X., Huang, Y., Zhao, P., Yang, Z., Gong, S., Wang, Z., 2023. Multimodal quantitative magnetic resonance imaging of the thalamus in tinnitus patients with different outcomes after sound therapy. CNS. Neurosci. Ther.

Chen, Y.C., Bo, F., Xia, W., Liu, S., Wang, P., Su, W., Xu, J.J., Xiong, Z., Yin, X., 2017a. Amygdala functional disconnection with the prefrontal-cingulate-temporal circuit in chronic tinnitus patients with depressive mood. Prog. Neuropsychopharmacol. Biol. Psychiatry 79, 249–257.

Chen, Y.C., Wang, F., Wang, J., Bo, F., Xia, W., Gu, J.P., Yin, X., 2017b. Resting-state brain abnormalities in chronic subjective tinnitus: a meta-analysis. Front. Hum. Neurosci. 11.

Chen, Y.C., Zhang, J., Li, X.W., Xia, W., Feng, X., Gao, B., Ju, S.H., Wang, J., Salvi, R., Teng, G.J., 2014. Aberrant spontaneous brain activity in chronic tinnitus patients revealed by resting-state functional MRI. Neuroimage-Clinical 6, 222–228.

Chen, Y.C., Xia, W., Luo, B., Muthaiah, V.P.K., Xiong, Z., Zhang, J., Wang, J., Salvi, R., Teng, G.J., 2015a. Frequency-specific alternations in the amplitude of low-frequency fluctuations in chronic tinnitus. Front. Neural Circuits. 9, Jan–J13.

Chen, Y.C., Zhang, J., Li, X.W., Xia, W., Feng, X., Qian, C., Yang, X.Y., Lu, C.Q., Wang, J., Salvi, R., Teng, G.J., 2015b. Altered intra- and interregional synchronization in resting-state cerebral networks associated with chronic tinnitus. Neural Plast. 2015, 475382.

De Ridder, D., Vanneste, S., Langguth, B., Llinas, R., 2015. Thalamocortical dysrhythmia: a theoretical update in tinnitus. Front. Neurol. 6, 124.

Friston, K.J., Ashburner, J., Kiebel, S., Nichols, T.E., Penny, W., 2007. Statistical parametric mapping: the analysis of functional brain images. In: Friston, Karl, Ashburner, John, Kiebel, Stefan, Nichols, Thomas, Penny, William (Eds.). Academic Press, Amsterdam.

Gault, R., McGinnity, T.M., Coleman, S., 2018. A Computational model of thalamocortical dysrhythmia in people with tinnitus. IEEe Trans. Neural Syst. Rehabil. Eng. 26, 1845–1857.

Hackenberg, B., O'Brien, K., Döge, J., Lackner, K.J., Beutel, M.E., Münzel, T., Pfeiffer, N., Schulz, A., Schmidtmann, I., Wild, P.S., Matthias, C., Bahr-Hamm, K., 2023. Tinnitus prevalence in the adult population-results from the gutenberg health study. Medicina (Kaunas) 59, 620.

Henry, J.A., Dennis, K.C., Schechter, M.A., 2005. General review of tinnitus: prevalence, mechanisms, effects, and management. J. Speech Lang Hear R 48, 1204–1235.

Jenkinson, M., Beckmann, C.F., Behrens, T.E., Woolrich, M.W., Smith, S.M., 2012. FSL. Neuroimage 62, 782–790.

Job, A., Jaroszynski, C., Kavounoudias, A., Jaillard, A., Delon-Martin, C., 2020. Functional connectivity in chronic nonbothersome tinnitus following acoustic trauma: a seed-based resting-state functional magnetic resonance imaging study. Brain Connect. 10, 279–291.

Khalfa, S., Dubal, S., Veuillet, E., Perez-Diaz, F., Jouvent, R., Collet, L., 2002. Psychometric normalization of a hyperacusis questionnaire. O.R.L. J. Oto-Rhino-Laryngol. Relat. Specialt. 64, 436–442.

Kok, T.E., Domingo, D., Hassan, J., Vuong, A., Hordacre, B., Clark, C., Katrakazas, P., Shekhawat, G.S., 2022. Resting-state networks in tinnitus. Clin. Neuroradiol. 32, 903–922.

Kok, T.E., Schaette, R., Shekhawat, G.S., 2021. Chapter 11 - Impact of tDCS and HD-tDCS on tinnitus perception: a scoping review. In: Langguth, B., Kleinjung, T., De Ridder, D., Schlee, W., Vanneste, S. (Eds.), Progress in brain research: tinnitus - an interdisciplinary approach towards individualized treatment: towards understanding the complexity of tinnitus. Elsevier.

Lefaucheur, J.P., 2016. A comprehensive database of published tDCS clinical trials (2005-2016). Neurophysiol. Clin. 46, 319–398.

Llinás, R.R., Ribary, U., Jeanmonod, D., Kronberg, E., Mitra, P.P., 1999. Thalamocortical dysrhythmia: a neurological and neuropsychiatric syndrome characterized by magnetoencephalography. Proceed. Nat. Acad. Sci. 96, 15222.

Maudoux, A., Lefebvre, P., Cabay, J.E., Demertzi, A., Vanhaudenhuyse, A., Laureys, S., Soddu, A., 2012. Auditory resting-state network connectivity in tinnitus: a functional MRI study. PLoS. One 7, e36222.

McCarthy, P., 2022. FSLeyes, 1.3.0 ed. Zenodo.

McCombe, A., Baguley, D., Coles, R., McKenna, L., McKinney, C., Windle-Taylor, P., 2001. Guidelines for the grading of tinnitus severity: the results of a working group commissioned by the british association of otolaryngologists, head and neck surgeons, 1999. Clinic. Otolaryngol. 26, 388–393.

Meikle, B.M., Henry, A.J., Griest, E.S., Stewart, J.B., Abrams, B.H., McArdle, J.R., Myers, W.P., Newman, C.C., Sandridge, L.S., Turk, J.D., Folmer, W.R., Frederick, P. E., House, E.J., Jacobson, H.G., Kinney, M.S., Martin, E.W., Nagler, A.S., Reich, A.G., Searchfield, A.G., Sweetow, A.R., Vernon, A.J., 2012. The tinnitus functional index: development of a new clinical measure for chronic, intrusive tinnitus. Ear Hear. 33, 153–176.

Molloy, K., Griffiths, T.D., Chait, M., Lavie, N., 2015. Inattentional deafness: visual load leads to time-specific suppression of auditory evoked responses. The J. Neurosci. 35, 16046.

Poldrack, R.A., Mumford, J.A., Nichols, T.E., 2011. Preprocessing fmri data. handbook of functional MRI data analysis. Cambridge University Press, Cambridge.

Rauschecker, J.P., Leaver, A.M., Mühlau, M., 2010. Tuning out the noise: limbic-auditory interactions in tinnitus. Neuron 66, 819–826.

Rauschecker, J.P., May, E.S., Maudoux, A., Ploner, M., 2015. Frontostriatal gating of tinnitus and chronic pain. Trends Cogn. Sci. 19, 567–578.

Schaette, R., Kempter, R., 2006. Development of tinnitus-related neuronal hyperactivity through homeostatic plasticity after hearing loss: a computational model. Eur. J. Neurosci. 23, 3124–3138.

Schmidt, S.A., Akrofi, K., Carpenter-Thompson, J.R., Husain, F.T., 2013. Default mode, dorsal attention and auditory resting state networks exhibit differential functional connectivity in tinnitus and hearing loss. PLoS. One 8, e76488.

Schmidt, S.A., Carpenter-Thompson, J., Husain, F.T., 2017. Connectivity of precuneus to the default mode and dorsal attention networks: a possible invariant marker of long-term tinnitus. Neuroimage Clin. 16, 196–204.

Smith, S.M., Jenkinson, M., Woolrich, M.W., Beckmann, C.F., Behrens, T.E., Johansen-Berg, H., Bannister, P.R., De Luca, M., Drobnjak, I., Flitney, D.E., Niazy, R.K., Saunders, J., Vickers, J., Zhang, Y., De Stefano, N., Brady, J.M., Matthews, P.M., 2004. Advances in functional and structural MR image analysis and implementation as FSL. Neuroimage 23 (Suppl 1), S208–S219.

Vanneste, S., Alsalman, O., De Ridder, D., 2019. Top-down and bottom-up regulated auditory phantom perception. J. Neurosci. 39, 364–378.

Vernon, J.A., Meikle, M.B., 2000. Tinnitus masking. In: Tyler, R.S. (Ed.), Tinnitus handbook. Singular Pub. Group, San Diego: San Diego.

Whitfield-Gabrieli, S., Nieto-Castanon, A., 2012. Conn: a functional connectivity toolbox for correlated and anticorrelated brain networks. Brain Connect. 2, 125–141.

Zhang, J., Chen, Y.C., Feng, X., Yang, M., Liu, B., Qian, C., Wang, J., Salvi, R., Teng, G.J., 2015. Impairments of thalamic resting-state functional connectivity in patients with chronic tinnitus. Eur. J. Article Radiol. 84, 1277–1284.

Zung, W.W.K., 1965. A self-rating depression scale. Arch. Gen. Psychiatry 12, 63–70.

Zung, W.W.K., 1971. A rating instrument for anxiety disorders. Psychosomatics (Washington, D.C.) 12, 371–379.